Astron. Astrophys. 133, 127–136 (1984)

ASTRONOMY AND ASTROPHYSICS

Distribution and motions of atomic hydrogen in lenticular galaxies
II. NGC 7013

G. R. Knapp[1,2], W. van Driel[2], U. J. Schwarz[2], H. van Woerden[2], and J. S. Gallagher III[3]

[1] Princeton University Observatory, Princeton, NJ 08544, USA
[2] Kapteyn Astronomical Institute, University of Groningen, NL-9700 AV Groningen, The Netherlands
[3] Department of Astronomy, University of Illinois, Urbana, IL 61801, USA

Received May 31, accepted October 27, 1983

Summary. The H I-rich SO/a galaxy NGC 7013 was mapped in the H I line with a spatial resolution of $25'' \times 50''$ ($\alpha \times \delta$) and a velocity resolution of 33 km s^{-1}. On the large scale, the H I distribution may be described by two rings, the larger at the edge of the optical disc and the smaller possibly associated with the inner stellar ring in the galaxy. The H I surface density in the disc itself is very low. We suggest that NGC 7013 is a former late-type spiral in which the H I density in the disc has become too low for significant star formation. The presence of the outer H I ring in the galaxy makes it unlikely that this is due to external sweeping.

Key words: lenticular galaxies – individual galaxies: NGC 7013 – interstellar medium: distribution and motions of H I

I. Introduction

This is Paper II in a series of studies of the H I distribution in lenticular (SO) galaxies carried out at the University of Groningen using the Westerbork Synthesis Radio Telescope (WSRT). The gas content of early-type galaxies is a subject of continuing current interest because of its importance in questions concerning the evolution of stellar populations of galaxies and the evolution of the energetic activity seen in the nuclei of some elliptical galaxies. In recent years, it has been found that there is a very wide range in the global gas content of galaxies which are otherwise morphologically similar. The observations of elliptical galaxies have been discussed by Sanders (1980) and Knapp (1983). Several recent surveys of the H I content of nearby SO galaxies have also been made (Bieging and Biermann, 1977; Knapp et al., 1977, 1978; Balkowski, 1979; Krumm and Salpeter, 1979a, b; Balkowski and Chamaraux, 1983; Gallagher et al., 1983; van Woerden et al., 1983b). These studies show that the H I content of SO galaxies varies over a very wide range, from an undetectable amount (the case for most lenticular galaxies) to values of M_H/L_B as high as those found for late-type spirals.

Several explanations have been offered for these results. Larson et al. (1980) have suggested that SOs are former spirals which have run out of interstellar gas, or which contain residual gas whose density is too low for efficient star formation. They point out that, for many of the large nearby spirals, the lifetime of the global gas content against the current star formation rate is quite short, only a few times 10^9 yr. Thus the existence of SOs may mean that some spirals are at the end of their star-forming lifetime (cf. Bothun, 1982). This possibility is supported by the finding by Butcher and Oemler (1978) of a significantly larger fraction of blue galaxies in the recent past, at distances of $z \gtrsim 0.4$.

On the other hand, the dominance of SOs over spirals in rich clusters of galaxies (e.g. Kent, 1981) suggests that the gas has been lost from cluster spirals by sweeping. In loose groups, the evolution of the gas content of early-type galaxies may go the other way; these galaxies may accrete H I from their late-type neighbours (Silk and Norman, 1979).

Of central importance to these questions is a knowledge of the distribution and motions of the H I in those SO galaxies containing significant atomic hydrogen. The systematic properties of the H I distribution in spiral galaxies have been studied for several years with the WSRT (see Bosma, 1981a, b). With the continued improvement of the sensitivity of this telescope, it has become possible to study galaxies with smaller H I emissivity, and the present series of papers describes synthesis observations of SO and SO/a galaxies. The problems to be examined in this programme, and some preliminary results, are described by Van Woerden et al. (1983a: Paper I). In the present paper, we discuss the distribution and dynamics of the H I in NGC 7013. This galaxy, usually classified as SO/a, is a bright nearby galaxy but has received little observational attention because it is quite close to the galactic plane ($b = -11°$) and hence is heavily obscured and confused. It is, however, one of the nearest SO galaxies with a strong H I signal (Balkowski et al., 1972; Gallagher et al., 1983) and is thus a good candidate for synthesis observations. We describe our H I-line synthesis observations of this galaxy in the next section; in Sect. III we describe the data reduction and results. The H I distribution and velocity field of the galaxy are discussed in Sect. IV, and the conclusions in Sect. V.

II. The observations

The 21-cm line observations descrvations described herein were made using the WSRT in the summer of 1979 in four sessions, with a total observing time of 18 h. A journal of the observations is given in Table 1a, and the instrumental and observational parameters in Table 1b. The digital line backend (Bos et al., 1981) was used to observe two polarizations in 31 channels over a bandwidth of 2.5 MHz; the resulting channel spacing is 16.6 km s^{-1}. The data were calibrated using standard continuum sources and Hanning smoothed in the line backend to give a resolution of $\sim$33 km s^{-1}. The velocities in this paper are heliocentric and calculated according to the conventional optical definition ($V = c\Delta\lambda/\lambda_0$). Bad data were edited out, and the combined data Fourier transformed

Send offprint requests to: G. R. Knapp

Table 1a. Journal of observations of NGC 7013

Observing dates	July 12, 1979 July 21, 1979	August 31, 1979 September 1, 1979
Total observing time	12^h	6.5^h
Baselines:	36, 72, 108, 144, ..., 1440 m[a]	72, 144, 216, 288, ..., 1584 m[b]
HA Coverage	$-90°$ to $-10°$ $-10°$ to $90°$	$-90°$ to $-38°$ $40°$ to $90°$

Table 1b. Instrumental parameters of the observations

Heliocentric radial velocity	781 km s^{-1}
Field centre coordinates, 1950	$21^h01^m24^s$; $+29°42'$
Primary beam (FWHM)	37.0
Synthesized beam ($\alpha \times \delta$)	$24''.8 \times 50''.1$
Total bandwidth	2.5 MHz
Velocity resolution	33 km s^{-1}
Channel spacing	16.6 km s^{-1}
RMS noise in channel maps	2.5 mJy/beam

[a] 40 Independent spacings

[b] 22 Independent spacings; spacings of 72, 144, 1512, 1584 m are not redundant

using the program LINEMAP at the Leiden computer centre to produce maps of the intensity distribution in each channel. The subsequent data reduction was carried out in Groningen, using the Groningen Image Processing System GIPSY (Shostak and Allen, 1980). The results obtained are in substantial agreement with those of earlier, incomplete observations by Schwarz and Van Woerden made with an angular resolution of $50'' \times 100''$ and a velocity resolution of ~ 40 km s^{-1}.

Table 2. Observed properties of NGC 7013

Optical position (1950)	$\alpha = 21^h01^m26^s.4 \pm 0^s.2$ $\delta = +29°41'55'' \pm 4''$
Type	SA(r)O/a (RC 2)
Distance	11.8 h^{-1} Mpc
Face on diameter $D(0)_{25}$	3.9
Linear diameter	13.4 h^{-1} kpc
Disc inclination	$72° \pm 5°$
Total corrected magnitude B_T^0	$11^m.18$
Corrected colour $(B-V)_T^0$	$+0^m.81$
$(U-B)_T^0$	$+0^m.18$
Total blue luminosity L_B^0	$7.4\,10^9$ h^{-2} $L_\odot$
Integrated H I flux	21.6 Jy km s^{-1}
H I mass M_{HI}	$7.1\,10^8$ h^{-2} $M_\odot$
H I diameter D_{100}	4.3
Heliocentric velocity V_{sys}	775 ± 20 km s^{-1}
H I profile widths $W_{0.2}$	336 ± 40 km s^{-1}
$W_{0.5}$	305 ± 40 km s^{-1}
Circular velocity V_c	170 ± 25 km s^{-1}
M_{HI}/L_B	0.1
Total mass M_T	$4.4\,10^{10}$ h^{-1} $M_\odot$
M_T/L_B	6.0 h $M_\odot/L_\odot$

III. The results

The optical and radio parameters derived for this galaxy are summarized in Table 2.

(a) The optical properties of the galaxy

NGC 7013 is classified as an SO/a galaxy with an inner ring (de Vaucouleurs et al., 1976, RC 2). Short exposure blue and Hα region pictures (Lynds, 1974; these are reproduced in Figs. 6 and 7) show a small central bulge (blue diameters 0.3×0.2) surrounded by a bright inner ring and a faint disk, both crossed by dust lanes. The major axis of the ring is at position angle 175°, and its diameters are 1.0×0.25. On the Hα print, the ring shows no strong condensations, and the galaxy spectrum shows no strong Hα or [O II] λ3727 Å emission (Lynds, 1974).

The longer-exposure pictures of the Palomar Observatory-National Geographic Sky Survey show an extended disc around the burned-out bulge and ring; the UGC (Nilson, 1973) gives a major axis position angle for the disc of 157° and blue diameters of 5.2×1.6.

The disc shows little structure, except for a faint, thin spiral-like feature, barely visible on both the long and short exposure photographs, which runs from the north of the ring, through east, into the south eastern disc. A second spiral feature on the opposite (north-west) side of the disc is visible on the Sky Survey picture.

The position of the optical center of the galaxy has been measured from the Sky Survey prints by Dressel and Condon (1976). Since the central regions of the galaxy are burnt out on the Sky Surveys images, we re-determined the position of the small central bulge using the pictures of Lynds (1974) and find the values for α and δ listed in Table 2. This position is about 6".5 away from that given by Dressel and Condon (1976), but agrees very well with that of Gallouët et al. (1973).

The isophotal diameter is $D(0) = 3.9$ (RC 2) after correction for inclination. The total observed blue magnitude of the galaxy is $B_T = 12.45$ and the colours are $(B-V)_T = 1.10$, $(U-B)_T = 0.46$ (de Vaucouleurs et al., 1978). These were corrected for internal extinction in the galaxy, for the redshift, and for foreground extinction in the Galaxy according to the prescriptions of the RC 2. The foreground extinction to the galaxy given by the model in the RC 2, $A_B = 0.98$, is about twice as high as that given by a simple cosecant law, but is confirmed using the H I column density from the surveys of Weaver and Williams (1974) and Heiles (1975) and $N_H/E_{B-V} = 5\,10^{21}$ cm^{-2} mag^{-1}. The axial ratio R_{25} given in the RC 2, together with an assumed true axial ratio of 0.2, gives an inclination $i = 72° \pm 5°$. The corrected magnitude and colours are then given in Table 2; the colours are fairly normal for an SO or Sa galaxy and show no evidence of strong current star formation.

The heliocentric radial velocity found from the H I line is 775 km s^{-1} (Sect. IIId). Correcting this for the solar motion with respect to the Local Group (from the RC 2) and for the motion of

the Local Group with respect to the Virgo Cluster (Tonry and Davis, 1981), and using a Hubble constant

$H_0 = 100\,h\,km\,s^{-1}\,Mpc^{-1}$,

the distance to NGC 7013 is $11.8\,h^{-1}$ Mpc. The isophotal diameter, corrected for inclination, is then $13.4\,h^{-1}$ kpc and the corrected blue luminosity $7.4\ 10^9\ h^{-2}\ L$. The optical properties of the galaxy are summarized in the first part of Table 2.

(b) Continuum sources

The field of NGC 7013 contains several radio sources, including two which are fairly strong (several hundred mJy). The grating rings produced by these sources were not satisfactorily removed from the line channel maps by continuum subtraction (see below). Because of this, the channel maps were first individually cleaned (Högbom, 1974) to remove these two sources. One is a complex extended source and the cleaning was not perfect outside the galaxy. There are minor residual effects of this source in the data.

The channel maps were then examined individually to find a velocity range clear of H I emission which could be used to determine the continuum. The first and last two channels were discarded since they were on the edge of the band and of low sensitivity. Channels 2, 3, 28, and 29 were found to be free of line emission and velocity-weighted average continuum maps made which were then subtracted from the corresponding line channel maps. The average continuum map showed a weak, unresolved source of strength $S(1417\,MHz) = 22 \pm 4$ mJy at the centre of the galaxy. This source, whose position is the first entry in Table 3, is coincident with the optical centre of the galaxy to within the errors. The intrinsic luminosity of the source is $P(1417\,MHz) = (3.6 \pm 0.6)\,10^{20}\,h^{-2}\,W\,Hz^{-1}$. No other continuum emission from the galaxy is apparent in the WSRT observations, with a limit of ~4 mJy/beam. Dressel and Condon (1978) find $S(2380\,MHz) = 14 \pm 3$ mJy in a beam $3' \times 3'$. The observations are thus consistent with the presence of a small non-thermal source of the type often found in the nuclei of early-type galaxies.

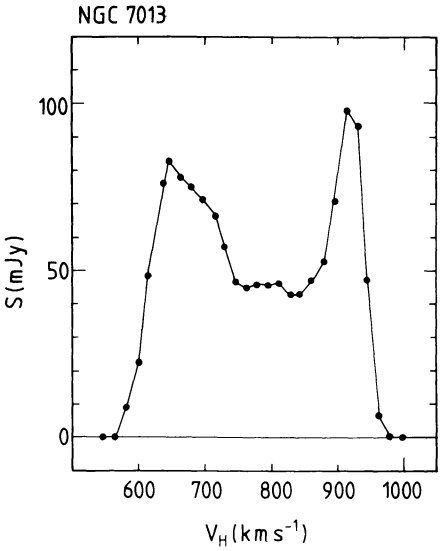

Fig. 1. Global H I profile for NGC 7013, measured with the WSRT

The fluxes, positions and angular sizes of the remaining sources in the field of NGC 7013 stronger than 10 mJy are also listed in Table 3. The sources with no accompanying size information are point sources to the accuracy of the measurements. The source fluxes are corrected for attenuation by the primary beam of the array, and the source parameters found by fitting an elliptical gaussian to the data. The shape parameters given for the extended sources are corrected for the shape of the synthesized beam.

Table 3. Continuum sources in the field of NGC 7013

Source	α(1950)	δ(1950)	S(mJy) (1417 MHz)	Notes
1	$21^h01^m26^s.7 \pm 0.2$	$+29°41'\ 58.5 \pm 5.4$	22.0 ± 4.2	(a)
2	21 00 50.5 ± 0.1	+29°54′ 51.8 ± 2.5	321	(b)
3	21 02 47.6 ± 0.8	+30 04 02.5 ± 4.0	52.1 ± 8.4	
4	21 02 54.7 ± 0.12	+29 39 05.2 ± 4.9	17.6 ± 3.9	
5	21 02 31.5 ± 1.0	+29 44 38.7 ± 7.9	24 ± 12	(c)
6	21 02 35.1 ± 0.1	+29 38 03.0 ± 2.6	232 ± 22	
7	21 02 49.4 ± 0.3	+29 24 27.3 ± 4.8	16.2 ± 5.4	
8	21 01 38.8 + 0.02	+29 44 16.5 ± 0.4	6.7 ± 1.2	
9	21 01 35.8 ± 0.04	+29 40 41.8 ± 2.8	23.6 ± 2.4	
10	21 01 38.4 ± 0.3	+29 37 07.3 ± 3.6	14.2 ± 2.4	(d)
11	21 01 20.3 ± 0.13	+29 45 49.8 ± 1.1	21.6 ± 2.6	
12	21 00 41.6 ± 0.06	+30 02 17.4 ± 6.9	20.5 ± 5.3	
13	21 00 21.2 ± 0.08	+29 49 53.1 ± 2.6	61.8 ± 6.7	
14	21 00 41.0 ± 0.07	+29 31 10.0 ± 2.7	72.4 ± 7.3	
15	21 00 35.4 ± 0.07	+29 28 03.7 ± 1.6	62.7 ± 5.7	(e)
16	21 00 38.2 ± 0.2	+29 20 02.5 ± 6.4	16.7 ± 4.3	

Notes to Table 3: (a) Nuclear source of galaxy. (b) Complex head-tail source: size ~1′. (c) Source extended: h.p.diameter 49″ × 21″ at position angle 66°. (d) Source extended: h.p.diameter 64″ × 34″ at position angle 0°. (e) Source extended: h.p.diameter 45″ × 32″ at position angle 180°

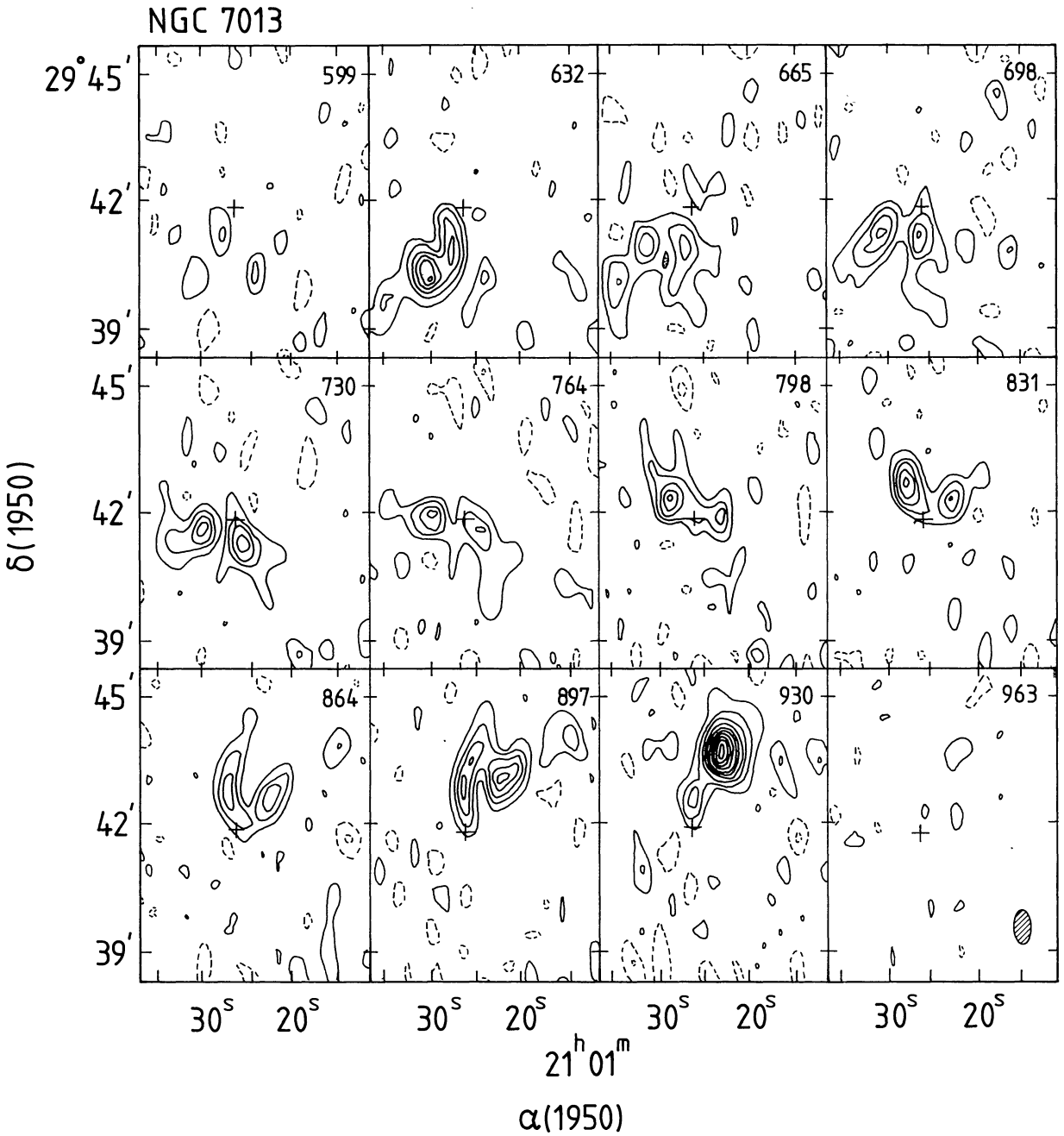

Fig. 2. Channel maps with a velocity spacing of 33 km s^{-1}, showing the distribution of the 21-cm line radiation for NGC 7013. The heliocentric velocity in km s^{-1} is given in the upper right-hand corner for each channel map; the velocity resolution is 33 km s^{-1}. The cross gives the position of the optical center of the galaxy. The maps are not corrected for the attenuation of the array primary beam. Negative contours are dashed and the zero-level contour is omitted. The contour intervals are 1.3 K, about three times the rms noise of each map. The cross-hatched ellipse gives the half-power size of the synthesized beam

(c) The global H I *profile and* H I *content of* NGC *7013*

The global H I profile was obtained by integration over the individual channel maps after continuum subtraction. Before the summation, the flux at each position was corrected for attenuation by the primary beam of the array. The resulting global profile is shown in Fig. 1 and has the two-horned appearance characteristic for emission from gas in a rotating disc. The observed parameters of the profile, including the total H I flux, are given in Table 2. $W_{0.2}$ is the profile width between the 20% power points and $W_{0.5}$ that between the 50% power points, both corrected for instrumental smoothing. These values agree within the errors with those found in observations with the NRAO 91-metre telescope (Gallagher et al., 1983), and with the Nançay telescope (Bottinelli et al., 1982) showing that little of the H I in NGC 7013 (no more than ~10%) is likely to be in very extended ($\gtrsim 5'$) structures.

The circular velocity in the disk of the galaxy is found from the H I profile width, corrected for inclination, to be ~170 km s^{-1}. This value of the circular velocity, together with the blue

luminosity of the galaxy, lie fairly close to the mean luminosity-velocity width relationship of Tully and Fisher (1977). The H I mass-to-blue-luminosity ratio is $M_{HI}/L_B = 0.095$, typical of an Sa galaxy (Shostak, 1978; Bottinelli et al., 1980; Huchtmeier, 1982). The circular velocity is, however, at the low end of the observed range for Sa galaxies.

(d) The H I surface density distribution and velocity field

In Fig. 2 is shown the distribution of the H I emission in the individual velocity channels; the line channel maps have had the continuum subtracted from them. The data show the characteristic velocity pattern of gas rotating in an inclined disc with a flat or rising rotation curve (Roberts, 1975).

The map of the distribution of total H I column density was constructed as follows. The individual channel maps were smoothed to a resolution of $90'' \times 90''$. The full-resolution channel maps were then added together using the full-resolution data wherever $T_B > 0.5$ K (2.5σ) in the smoothed maps, and setting $T_B = 0$ elsewhere. The resulting map is shown in Fig. 3 (upper panel).

Figure 3 shows an unusual distribution of H I, with regions of low H I surface density near the centre of the galaxy and in the disc. Because of this distribution, some care was taken in constructing the velocity field, and three different methods were used. First, the line profiles were drawn for each pixel (spacing $11'' \times 22''$ in α and δ), and the mean velocity estimated by eye to about half a channel. In almost all cases, the lines are strong and have velocity widths close to the velocity resolution of the observations. An interpolated contour map of the mean velocities was then made. Second, a similar map was made using computer-calculated intensity-weighted mean velocities of all profiles. Third, a gaussian was fitted to the line profile at each pixel and the resulting mean velocities interpolated to construct a velocity contour map. The differences among the three maps were mostly less then about half of the velocity resolution.

The contour map of the gaussian-fitted mean velocity is presented in Fig. 3, lower panel. The outer contours of the velocity map show little sign of the bending which characterizes large-scale warps, so that the H I disc seems to be fairly flat. However, the inner contours are twisted, and the kinematic major and minor axes skewed relative to each other. This is discussed in Sect. IV.

(e) Comparison of the H I distribution and velocity field with the optical appearance of the galaxy

The derived H I distribution and velocity field of the galaxy are compared with optical images in Figs. 4–7. In Figs. 4 and 5, the distributions are shown compared with the red sky survey prints, and in Figs. 6 and 7 with the blue photograph of Lynds (1974).

The distribution of H I column density in the galaxy is unusual; instead of the more-or-less steady decline of H I surface density with increasing radius seen in the discs of most spirals (Bosma, 1981a), the H I distribution shows several pronounced maxima and minima. There is an unresolved minimum close (20″ E) to the centre, and two deep minima at ~1′ NW and ~1.2 SE of the centre, in the disc of the galaxy.

There are several bright maxima in the H I distribution, the brightest, 0.5 north of the centre, having a column density $N_{HI} > 16\,10^{20}$ cm^{-2}, and hence a surface density perpendicular to the disk of $> 5\,10^{20}$ cm^{-2}. Several other maxima, with $N_{HI} \sim 9$–$12\,10^{20}$ cm^{-2}, are apparent in the H I map. Most of these maxima fall close to the weak structure seen optically in the disc, described in Sect. IIIa above. Hence, there is a hint of azimuthal asymmetry (residual spiral structure?) in both the H I and light distributions.

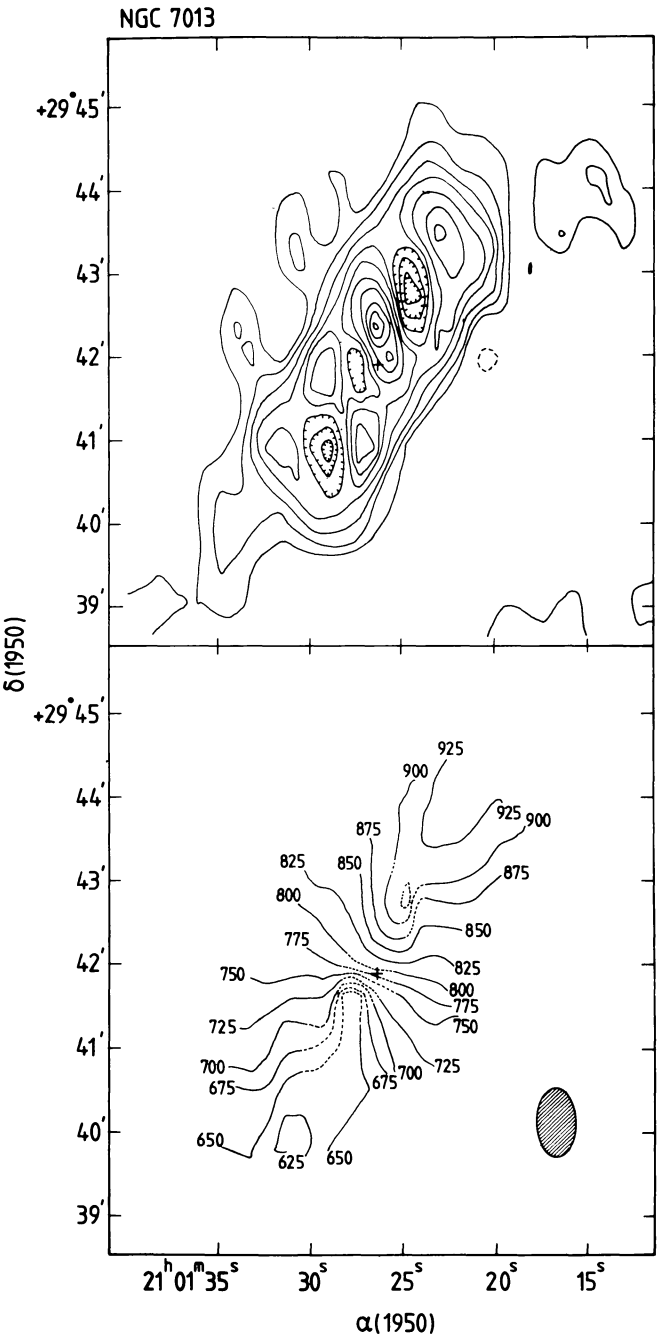

Fig. 3. Distribution of H I column density (upper panel) and velocity field (lower panel) for NGC 7013. The cross gives the position of the optical center of the galaxy, and the cross-hatched ellipse the size of the synthesized beam. For the H I column density, negative contours are dashed and minima are indicated by hatched contours. The zero-level contour is not plotted. The contour interval is $1.65\,10^{20}$ cm^{-2}, equivalent to $0.5\,10^{20}$ cm^{-2} in surface density perpendicular to the galactic disc. For the velocity field, the labels on the contours indicate the heliocentric velocity in km s^{-1}. The velocity contours are dashed where the H I column density is low and the velocity field correspondingly uncertain

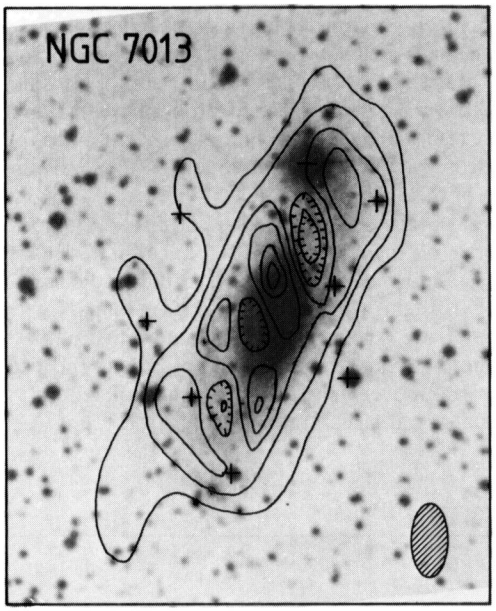

Fig. 4. H I column density distribution for NGC 7013 superimposed on a copy of the red print from the Palomar Sky Survey. © 1960 National Geographic – Palomar Sky Survey. Reproduced by permission of the California Institute of Technology. The contour interval is $2.3\,10^{20}\,\mathrm{cm}^{-2}$; the zero-level contour is omitted

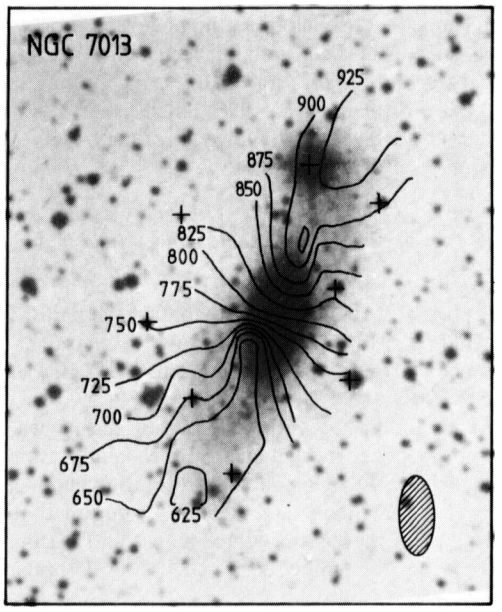

Fig. 5. H I velocity field for NGC 7013 superimposed on a copy of the red print from the Palomar Sky Survey © 1960 National Geographic – Palomar Sky Survey. Reproduced by permission of the California Institute of Technology

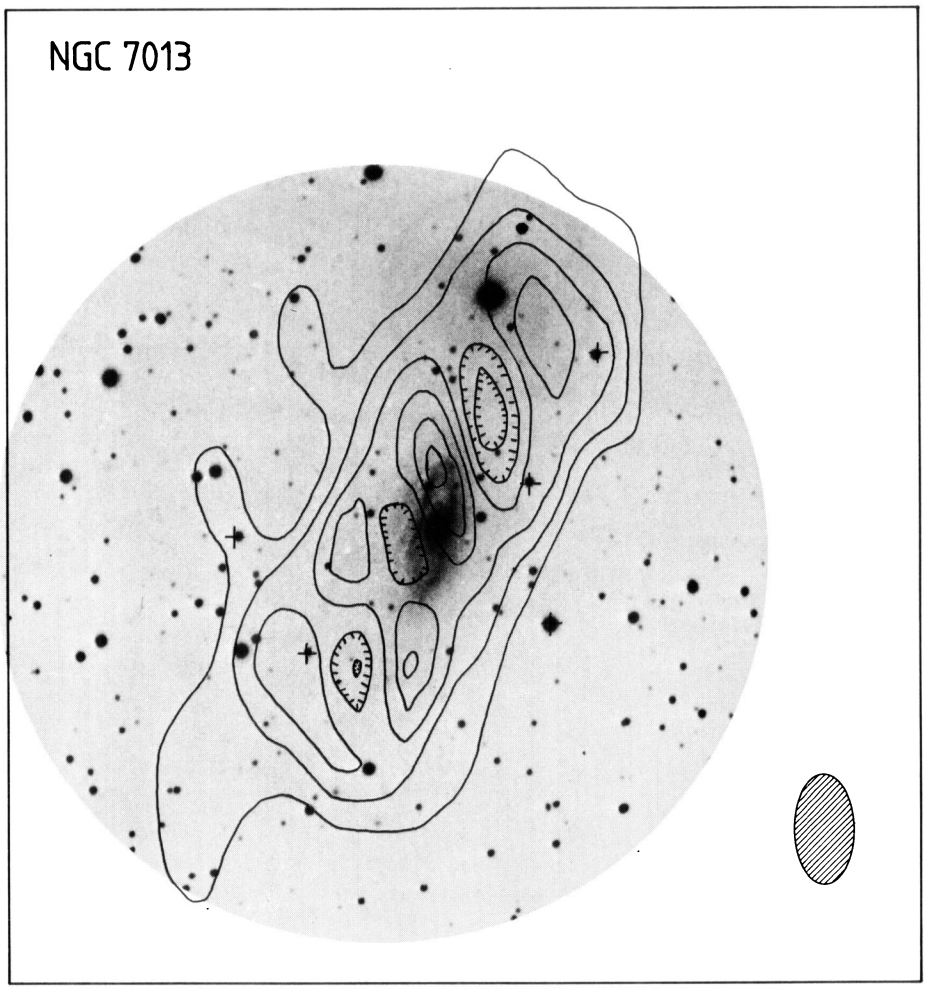

Fig. 6. H I column density distribution for NGC 7013 superimposed on a short-exposure blue (λ 4300 Å) photograph of the galaxy (Lynds, 1974). The contour values are as in Fig. 4

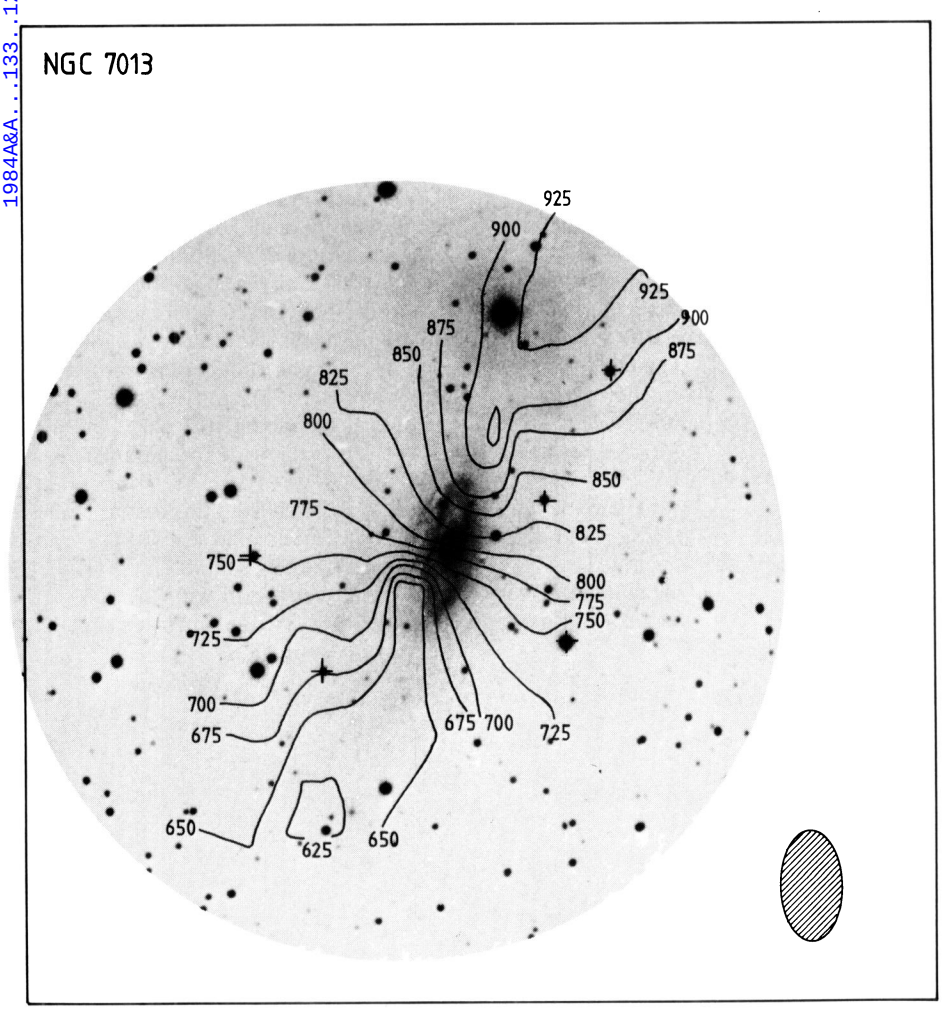

Fig. 7. H I velocity field for NGC 7013 superimposed on the blue photograph of the galaxy (cf. Fig. 6)

On a large scale, the H I extent of the galaxy is roughly comparable to that of the optical disc. In the next section, the distribution of H I in the disc is investigated by the construction of simple models.

(f) The mass and mass-to-light ratio

NGC 7013 has a relatively low rotation velocity for an early-type galaxy, and a comparison with the rotation velocities of Sb galaxies (Rubin et al., 1982) and SO galaxies (Dressler and Sandage, 1983) shows that, in this property, it is more similar to typical spirals than to more luminous Sa and SO galaxies (see also Bottinelli et al., 1980; Huchtmeier, 1982). Taking an optical radius of $6.7\,h^{-1}$ kpc (cf. Table 2), the estimated mass for a spherical distribution within the optical radius is $4.4\,10^{10}\,h^{-1}\,M_\odot$ and the mass-to-light ratio $6.0\,h\,M_\odot/L_\odot$. This puts NGC 7013 at the low end of the range of M/L for Sa systems, and again indicates a structural similarity with smaller spirals, which also tend to have low values of M/L.

IV. The H I distribution in NGC 7013

(a) A two-ring model

The nature of the H I distribution in NGC 7013 was first investigated via the examination of simple axisymmetric models. The approach used in constructing these models is similar to that of Rogstad et al. (1974) and Bosma (1981b). That is, the H I is assumed to be distributed in a series of concentric annuli, each with its own value of surface density σ(H I), inclination to the line of sight i, and position angle of the major axis Ψ. The projection on the sky of the H I surface density of the model is then calculated, smoothed by the synthesized beam of the observations, and compared with the observed maps.

In the case of NGC 7013 the peculiarities of the distribution are hinted at by the H I column density map (Fig. 3), which suggests that much of the H I lies in two rings. This is further demonstrated by Figs. 8 and 9. Figure 8 is a position-velocity map at position angle = 150°, close to the major axis of NGC 7013. On such maps, each ring in the galaxy becomes a line whose slope depends on its radius and rotation velocity. Figure 8 suggests the presence of two such rings, with little gas in between. The rings appear to be not quite symmetric with respect to the optical centre of the galaxy. In Fig. 9, we show the radial distribution of H I column density in NGC 7013. In the upper panel is shown the mean column density averaged in elliptical rings, and in the lower panel the mean distribution along the major axis. The differences between these two distributions can be attributed to the overlapping of the inner and outer H I features, as projected on the sky and smeared by the telescope beam.

Accordingly, a two-ring model of NGC 7013 was made, and the values of i, Ψ, ring radius and ring surface densities σ (H I)

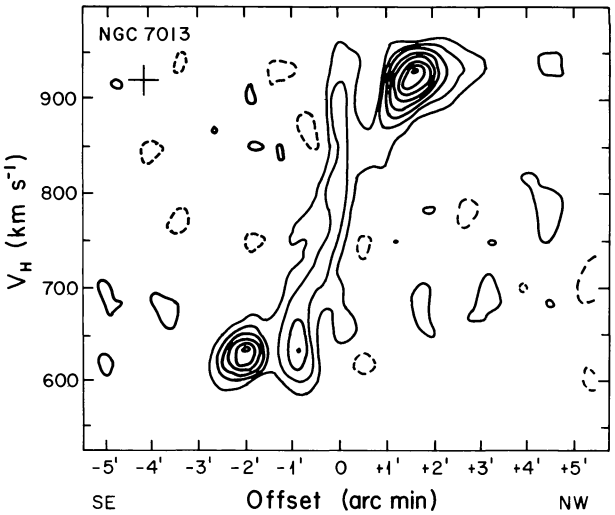

Fig. 8. Intensity as a function of velocity and position at position angle 150° for NGC 7013. Negative contours are dotted. The contour interval is 1.2 K, and the zero-level contour is not shown. The resolution is shown by a cross

varied. The resulting model map was convolved with a gaussian beam of the same dimensions as the observational synthesized beam, and the input parameters varied until reasonable correspondence with the observed distribution was found. The best-fit parameters are summarized in Table 4 and illustrated in Fig. 9. Models providing reasonably close fits to the data had similar properties; (1) the gas is distributed in two unresolved rings, the outer having lower H I surface density than the inner; (2) a slightly better fit is found if a disc of low surface density is added; (3) all of the components seem to fit reasonably well to the observed inclination of the optical body (72°) but the plane of the inner ring makes an angle of about 20° to the plane of the outer ring and disk. The fitted values of i and Ψ have an uncertainty of about 5°. The position angles of the inner and outer H I rings (175°, 150°) agree closely with those of the optical inner ring (175°) and the disc (157°). The model surface density map with the parameters of Table 4 is shown in Fig. 10.

The velocity field was then calculated from this best fit model. It was assumed that the rotation curve is flat at 170 km s^{-1}, as suggested by Fig. 8. The calculated velocity field was multiplied by the column density and the result convolved with the telescope beam. This map was then divided by the intensity map, to

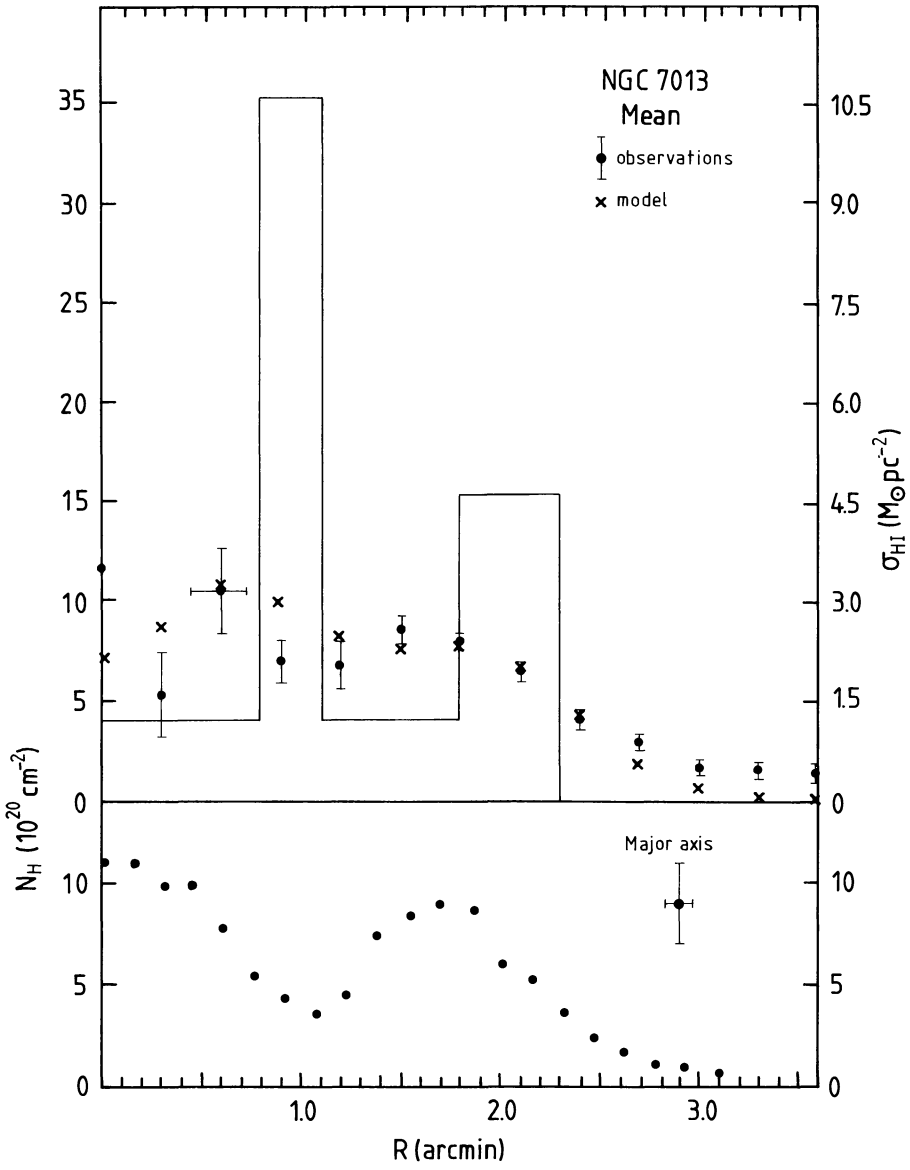

Fig. 9. Variation of H I column density in NGC 7013 with radius. Upper panel dots: measured from the total H I map (Fig. 3) by averaging the brightness in elliptical rings centered on the position of the galaxy, at position angle 150°, and with an eccentricity corresponding to an inclination of 68°. Lower panel: column density distribution along the major axis averaged on both sides of the centre. The bars in the upper right indicate the error and axis spacing of each point. The upper panel also shows the distribution of (face-on) surface density σ(H I) in the tilted-ring model of Table 4 (histogram, scale at right), and the corresponding distribution of beam-smeared column density N_H in the sky (crosses)

Table 4. Tilted-ring model for the H I distribution in NGC 7013

Ring	Inner ring	Outer ring	Disc
Inner radius (kpc)	$2.7\,h^{-1}$	$6.2\,h^{-1}$	0
Outer radius (kpc)	$3.8\,h^{-1}$	$7.9\,h^{-1}$	$7.9\,h^{-1}$
H I surface density, σ(H I) ($M_\odot$ pc^{-2})	9.4	3.5	1.2
Inclination i(°)	68 ± 5	68 ± 5	68 ± 5
Position angle Ψ(°)	175 ± 5	150 ± 5	150 ± 5
H I mass $M_{\rm HI}$ ($M_\odot$)	$2.1\,10^8\,h^{-2}$	$2.7\,10^8\,h^{-2}$	$2.3\,10^8\,h^{-2}$

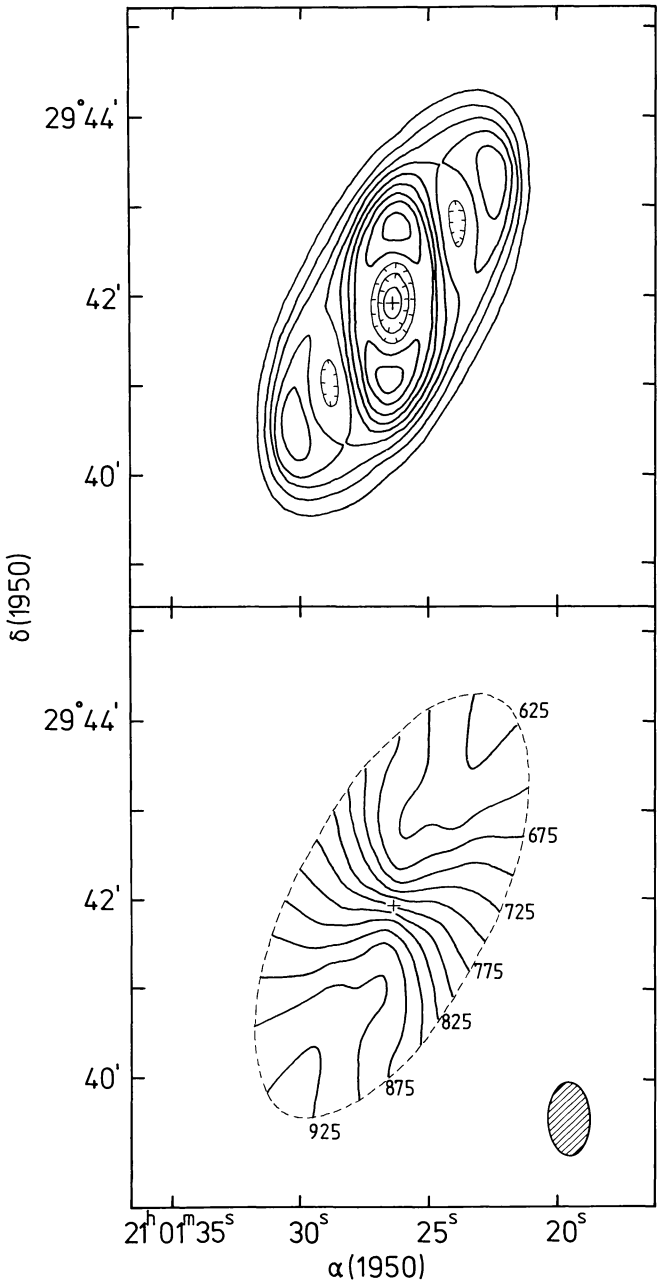

Fig. 10. Model H I column density distribution (upper panel) and velocity field (lower panel) for NGC 7013 (see text). The contour interval for the column density map is $1.5\,10^{20}$ cm^{-2}

approximate the processes involved in acquiring and reducing the data. This model velocity field is also shown in Fig. 10.

A comparison of the model and observed column density distributions (Figs. 10 and 3, cf. also Fig. 9) shows that, on the large scale, the model reproduces the observed distribution quite well. The observed H I distribution is asymmetric in detail, however. The centre of symmetry of the observed distribution is displaced eastwards from the nucleus of the galaxy by about 15″; hence an improved fit could be obtained by centring the model distribution about 15″ east of the nucleus. Also, the H I intensities in the NW of the disc are higher than those in the SE (this is apparent also from the H I global profile, Fig. 1, and the channel maps, Fig. 2).

The agreement between the model and observed velocity fields (Figs. 10 and 3) is also fairly good on the large scale. Differences of order 25 km s^{-1} occur in limited regions, expecially E and SE of the centre. These differences can partly be understood as beam-smeared effects of the asymmetries in the density distribution. In the inner parts of the galaxy, the observed kinematic major and minor axes appear skewed with respect to each other, which may be due to non-circular motions and the presence of an oval distortion in the potential field (cf. Bosma, 1981a). However, we cannot draw firm conclusions about the presence of such motions because of the limited observational resolution.

We conclude that the observed H I distribution and motions are well represented by a tilted-ring model whose geometric properties agree with the optical structure of the galaxy.

(b) Properties of the H I *distribution*

Bosma (1981b) defines the relative sizes of the H I and optical discs via the ratio $D_{100}/D(0)$, where D_{100} is the diameter at which the H I surface density is $1.82\,10^{20}$ cm^{-2} (100 K km s^{-1} emissivity in the H I line) and $D(0)$ the face-on isophotal diameter (statistically corrected for internal extinction, but not for extinction in the Galaxy) taken from the RC 2. For NGC 7013, the value of σ(H I) $=1.82\,10^{20}$ cm^{-2} lies at 4.′5 (Fig. 9), while $D(0)=3.'9$. Thus $D_{100}/D(0)=1.1$, which lies at the low end of the range found by Bosma (1981b) for a sample of 21 spiral galaxies.

In the disc of NGC 7013, the best-fitting model H I face-on surface density is $\sim 1.2\,M_\odot$ pc^{-2} (Table 4). In our Galaxy, this surface density is found beyond about 15 kpc (Gordon and Burton, 1976) where star formation is not taking place to any significant extent. The outer ring has a somewhat higher mean surface density than this ($\sim 4\,M_\odot$ pc^{-2}), similar to that in the solar neighbourhood. The inner H I ring has a much higher mean surface density of gas, about $9\,M_\odot$ pc^{-2}, where this is a lower limit because the ring may also contain molecular gas (if the ring is wider than the assumed 0.′3, the gas density is correspondingly reduced).

V. Discussion and conclusions

The maps of NGC 7013 described above give information about the internal peculiarities of the galaxy itself, and possible about SOs as a class. The gas distribution and motions are fairly well represented by a tilted-ring model with parameters consistent with the optical morphology. The orientation of the inner H I ring agrees with that of the inclined optical inner ring, but it has a larger radius. It is difficult to understand the apparent lack of current star formation in the inner H I ring, which has both a surface density and a mass comparable to that of the inner regions of our galactic disc.

The outer gas structure in NGC 7013 does not have an optical counterpart, and may simply be the outer remains of the H I disc.

The low level of the gas density in the disk of NGC 7013, and the red colours of the galaxy, suggest that the gas content of the galactic disc has fallen below the threshold at which significant star formation is likely to take place. The presence of the outer H I structure makes it very unlikely that this is due to external sweeping. The small bulge-to-disk ratio and small rotation velocity show that NGC 7013 is a low-mass, low-density galaxy, unlike the more luminous, "standard" SOs (Dressler and Sandage, 1983). The galaxy may thus be a former late-type spiral which has exhausted most of its gas, either by star formation or by internal sweeping.

Acknowledgements. We thank the staff of the WSRT for their help with the observations, and Dr. B. T. Lynds for copies of the photographs used in Figs. 6 and 7. G. K. is very grateful to the Z.W.O. for a visiting fellowship to the University of Groningen and to the members of the Kapteyn Laboratory for their warm hospitality. Partial support for this work was provided by the National Science Foundation via grants AST-8009252 and AST-8213292 to Princeton University and by NATO grant RD No. 098.82. The Westerbork Radio Observatory is operated by the Netherlands Foundation for Radio Astronomy with the financial support of the Netherlands Organization for the Advancement of Pure Research (ZWO). W.V.D. is supported by ZWO through the Astron foundation.

References

Balkowski, C.: 1979, *Astron. Astrophys.* **78**, 190
Balkowski, C., Chamaraux, P.: 1983, *Astron. Astrophys. Suppl.* **51**, 331
Balkowski, C., Bottinelli, L., Gouguenheim, L., Heidmann, J.: 1972, *Astron. Astrophys.* **21**, 303
Bieging, J.H., Biermann, P.: 1977, *Astron. Astrophys.* **60**, 361
Bos, A., Raimond, E., van Someren Greve, H.W.: 1981, *Astron. Astrophys.* **98**, 251
Bosma, A.: 1981a, *Astron. J.* **86**, 1791
Bosma, A.: 1981b, *Astron. J.* **86**, 1825
Bothun, G.D.: 1982, *Astrophys. J. Suppl.* **50**, 39
Bottinelli, L., Gouguenheim, L., Paturel, G.: 1980, *Astron. Astrophys.* **88**, 32
Bottinelli, L., Gouguenheim, L., Paturel, G.: 1982, *Astron. Astrophys. Suppl.* **47**, 171
Butcher, H., Oemler, A.G.: 1978, *Astrophys. J.* **219**, 18
Dressel, L.L., Condon, J.J.: 1976, *Astrophys. J. Suppl.* **31**, 187
Dressel, L.L., Condon, J.J.: 1978, *Astrophys. J. Suppl.* **36**, 53
Dressler, A., Sandage, A.: 1983, *Astrophys. J.* **265**, 664
Gallagher, J.S., Bushouse, H., Knapp, G.R., Faber, S.M.: 1983 (in preparation)
Gallouët, L., Heidmann, N., Dampierre, F.: 1973, *Astron. Astrophys. Suppl.* **12**, 89
Gordon, M.A., Burton, W.B.: 1976, *Astrophys. J.* **208**, 346
Heiles, C.E.: 1975, *Astron. Astrophys. Suppl.* **20**, 37
Högbom, J.A.: 1974, *Astron. Astrophys. Suppl.* **15**, 417
Huchtmeier, W.K.: 1982, *Astron. Astrophys.* **110**, 121
Kent, S.M.: 1981, *Astrophys. J.* **245**, 805
Knapp, G.R.: 1983, in *Internal Kinematics and Dynamics of Galaxies*, IAU *Symp. 100*, ed. E. Athanassoula, Reidel, Dordrecht, p. 297
Knapp, G.R., Gallagher, J.S., Faber, S.M., Balick, B.: 1977, *Astron. J.* **82**, 106
Knapp, G.R., Kerr, F.J., Williams, B.A.: 1978, *Astrophys. J.* **222**, 800
Krumm, N., Salpeter, E.E.: 1979a, *Astrophys. J.* **227**, 776
Krumm, N., Salpeter, E.E.: 1979b, *Astrophys. J.* **228**, 64
Larson, R.B., Tinsley, B.M., Caldwell, C.N.: 1980, *Astrophys. J.* **237**, 692
Lynds, B.T.: 1974, *Astrophys. J. Suppl.* **28**, 391
Nilson, P.: 1973, Uppsala General Catalogue of Galaxies, *Uppsala Astron. Obs. Ann.* **6** (UGC).
Roberts, M.S.: 1975, in *Galaxies and the Universe*, eds. A. Sandage, M. Sandage, J. Kristian, University of Chicago Press, p. 309
Rogstad, D.H., Lockhart, I.A., Wright, M.C.H.: 1974, *Astrophys. J.* **193**, 309
Rubin, V.C., Ford, W.K., Thonnard, N., Burstein, D.: 1982, *Astrophys. J.* **261**, 439
Sanders, R.H.: 1980, *Astrophys. J.* **242**, 931
Shostak, G.S., Allen, R.J.: 1980, in *Proceedings of* ESO *Workshop on Two Dimensional Photometry*, ed. P. Crane, K. Kjär, p. 169
Shostak, G.S.: 1978, *Astron. Astrophys.* **68**, 321
Silk, J., Norman, C.A.: 1979, *Astrophys. J.* **234**, 86
Tonry, J.L., Davis, M.: 1981, *Astrophys. J.* **246**, 680
Tully, R.B., Fisher, J.R.: 1977, *Astron. Astrophys.* **54**, 661
de Vaucouleurs, G., de Vaucouleurs, A., Corwin, H.C.: 1978, *Astron. J.* **83**, 1331
de Vaucouleurs, G., de Vaucouleurs, A., Corwin, H.C.: 1976, Second Reference Catalogue of Bright Galaxies, University of Teyas Press, Austin (RC 2)
Weaver, H., Williams, D.R.W.: 1974, *Astron. Astrophys. Suppl.* **17**, 251
Van Woerden, H., Van Driel, W., Schwarz, U.J.: 1983a, in *Internal Kinematics and Dynamics of Galaxies*, IAU *Symp. 100*, ed. E. Athanassoula, Reidel, p. 99 (Paper I)
Van Woerden, H., Hawarden, T.G., Mebold, U., Goss, W.M., Siegman, B.: 1983b (in preparation)